

Optical Engineering

OpticalEngineering.SPIEDigitalLibrary.org

Efficient processing of reaction-sintered silicon carbide by anodically oxidation-assisted polishing

Qunzhang Tu
Xinmin Shen
Jianzhao Zhou
Xiaohui He
Kazuya Yamamura

Efficient processing of reaction-sintered silicon carbide by anodically oxidation-assisted polishing

Qunzhang Tu,^a Xinmin Shen,^{a,*} Jianzhao Zhou,^a Xiaohui He,^a and Kazuya Yamamura^b

^aPLA University of Science and Technology, College of Field Engineering, Research Center for Mechanical and Electrical Engineering, Haifu Street, Nanjing, Jiangsu 210007, China

^bOsaka University, Graduate School of Engineering, Research Center for Ultra-Precision Science and Technology, 2-1 Yamadaoka, Suita, Osaka 565-0871, Japan

Abstract. Reaction-sintered silicon carbide (RS-SiC) is a promising optical material for the space telescope systems. Anodically oxidation-assisted polishing is a method to machine RS-SiC. The electrolyte used in this study is a mixture of hydrogen peroxide (H_2O_2) and hydrochloric acid (HCl), and the oxidation potential has two modes: constant potential and high-frequency-square-wave potential. Oxide morphologies are compared by scanning electron microscope/energy dispersive x-ray spectroscopy and scanning white-light interferometer. The results indicate that anodic oxidation under constant potential can not only obtain a relatively smooth surface but also be propitious to obtain high material removal rate. The oxidation depth in anodic oxidation under constant potential is calculated by comparing surface morphologies before and after hydrofluoric acid etching. The theoretical oxidation rate is 5.3 nm/s based on the linear Deal–Grove model. Polishing of the oxidized RS-SiC is conducted to validate the machinability of the oxide layer. The obtained surface roughness root-mean-square is around 4.5 nm. Thus, anodically oxidation-assisted polishing can be considered as an efficient method, which can fill the performance gap between the rough figuring and fine finishing of RS-SiC. It can improve the machining quality of RS-SiC parts and promote the application of RS-SiC products. © The Authors. Published by SPIE under a Creative Commons Attribution 3.0 Unported License. Distribution or reproduction of this work in whole or in part requires full attribution of the original publication, including its DOI. [DOI: [10.1117/1.OE.54.10.105113](https://doi.org/10.1117/1.OE.54.10.105113)]

Keywords: reaction-sintered silicon carbide; anodically oxidation-assisted polishing; linear Deal–Grove model; oxidation rate; material removal rate; surface roughness.

Paper 150866 received Jul. 2, 2015; accepted for publication Sep. 29, 2015; published online Oct. 22, 2015.

1 Introduction

Reaction-sintered silicon carbide (RS-SiC) is a promising material for making optical mirrors in space telescope systems due to its excellent physical, mechanical, and chemical properties.^{1–3} With the increasing standard for ultrasmooth surface finishing and the demand for high material removal rate (MRR) in the machining of RS-SiC substrate, methods for processing RS-SiC have become the research focus in the fields of optics and ceramics.^{4,5} However, RS-SiC is a known difficult-to-machine material because of its high hardness and chemical inertness.³ These properties make it inefficient to process RS-SiC with traditional mechanical or chemical methods, such as diamond turning^{6,7} or plasma chemical vaporization machining (PCVM).⁸ Meanwhile, the RS-SiC substrate is mainly composed of SiC and Si.^{9,10} Thus, the differences in physical hardness and chemical activity between the nonuniform SiC grains and Si grains make the homogeneous removal of RS-SiC almost impossible.¹¹ Therefore, a novel method for processing RS-SiC is urgently demanded to increase the MRR in the rough figuring process and to improve the surface quality in the fine finishing process.

In this research, a novel processing method, named anodically oxidation-assisted polishing, is proposed for the

efficient machining of RS-SiC substrate. The method includes two important steps: generation of oxide layer on the RS-SiC surface by means of anodic oxidation and the validation of machinability of the oxidized RS-SiC sample by subsequently polishing the oxide using traditional ceria slurry abrasive. Anodic oxidation is a classical method for surface modification.^{3,12} The electrolyte used in anodic oxidation of RS-SiC, which consists of hydrogen peroxide (H_2O_2) and hydrochloric acid (HCl), has been proven as an effective oxidant to oxidize SiC specimen.^{13,14} The anodic oxidation system is constructed to generate an oxide layer on RS-SiC, while a ceria slurry polishing system is built to verify the machinability of the oxide. The potential used in anodic oxidation of RS-SiC has two modes: constant potential and high-frequency-square-wave (HFSW) potential. The oxide morphologies obtained in the two oxidation modes are compared by the scanning electron microscope/energy dispersive x-ray spectroscopy (SEM-EDX) observation and the scanning white-light interferometer (SWLI) detection. Afterward, the anodic oxidation depth of RS-SiC corresponding to a certain oxidation time in the constant potential mode is calculated by comparing the surface morphologies before and after the hydrofluoric acid (HF) etching. The oxidation rate is calculated based on the linear Deal–Grove model. Through tracing the surface qualities by the SWLI measurement after abrasive polishing for a certain time, the machinability of the oxide layer, which is obtained by anodic oxidation of RS-SiC, is validated.

*Address all correspondence to: Xinmin Shen, E-mail: shenxmjfgdx2014@163.com

2 Experimental Setup

The system for anodic oxidation of RS-SiC in the constant potential mode is shown in Fig. 1(a)³ and that for anodic oxidation of RS-SiC in the HFSW potential mode is shown in Fig. 1(b). The parameters in anodic oxidation under constant potential are summarized in Table 1³ and those in anodic oxidation under HFSW potential are summarized in Table 2. Afterward, the oxidized RS-SiC sample is investigated by SEM-EDX observation and SWLI detection, and it is used to evaluate the two oxidation modes.

In order to make a fair comparison of the oxide morphologies obtained in the two oxidation modes, the equivalent oxidation potentials in both anodic oxidation modes are both set to 9.8 V. Meanwhile, the oxidation time for both cases is also set to be the same (2 min).

3 Analysis of Oxide Morphologies

The oxidized RS-SiC samples in the two anodic oxidation modes are investigated by SEM-EDX observation. The obtained results are shown in Figs. 2 and 3, respectively. The surface morphologies before and after oxidation at the same position under constant potential are shown in Figs. 2(a) and 2(b) and those under HFSW potential are shown in Figs. 3(a) and 3(b). On the original RS-SiC surface, the SiC grains and Si grains are identified by SEM-EDX, and the representative grains are marked in Figs. 2(a) and 3(a). It can be seen that both the RS-SiC samples are oxidized entirely in the two modes, since there is no carbon element detected on the surface of the oxidized RS-SiC samples in Figs. 2(d) and 3(d). However, the oxide morphologies generated in the two anodic oxidation modes are different. In the constant potential mode, as shown in Figs. 2(b) and 2(c), there are protuberances and cracks on the oxidized RS-SiC sample. The oxidation rate among different SiC grains and Si grains is also different, which can be judged from the

Table 1 Anodic oxidation parameters under constant potential mode.

Oxidation potential	9.8 V (constant)
Cathode	Pt
Reference electrode	Ag/AgCl
Electrolyte	H ₂ O:H ₂ O ₂ (30 wt%): HCl (35 wt%) = 200 g:50 g:5 g
Anode	RS-SiC sample

Note: RS-SiC, reaction-sintered silicon carbide.

Table 2 Anodic oxidation parameters under high-frequency-square-wave potential mode.

Oxidation potential	19.6 V (square wave)
Duty ratio	50%
Frequency	20 KHz
Cathode	Pt
Electrolyte	H ₂ O:H ₂ O ₂ (30 wt%): HCl (35 wt%) = 200 g: 50 g: 5 g
Anode	RS-SiC sample

oxygen distribution in Fig. 2(e). In the HFSW potential mode, as shown in Figs. 3(b) and 3(c), there are holes and ditches on the oxidized RS-SiC. Also, it is difficult to identify the differences of oxidation rates among the initial SiC grains and Si grains from the oxygen distribution in

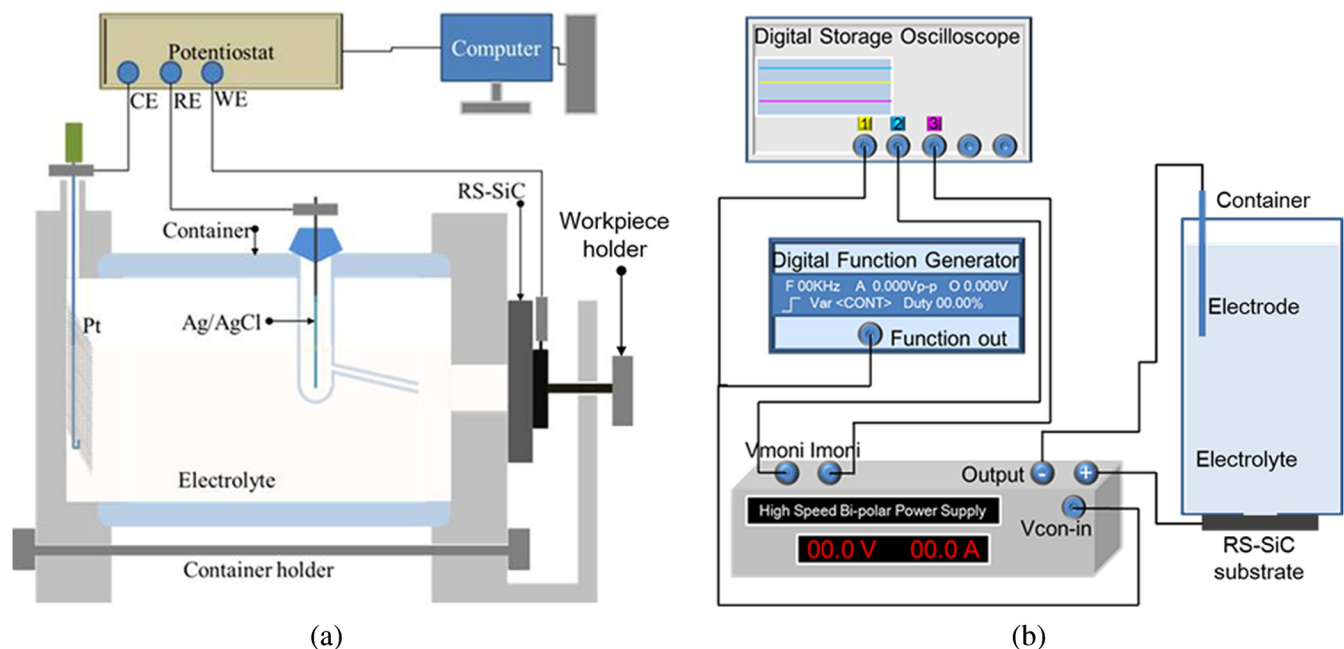


Fig. 1 Schematic diagram of the applied anodic oxidation systems: (a) anodic oxidation under constant potential mode and (b) anodic oxidation under high-frequency-square-wave (HFSW) potential mode.

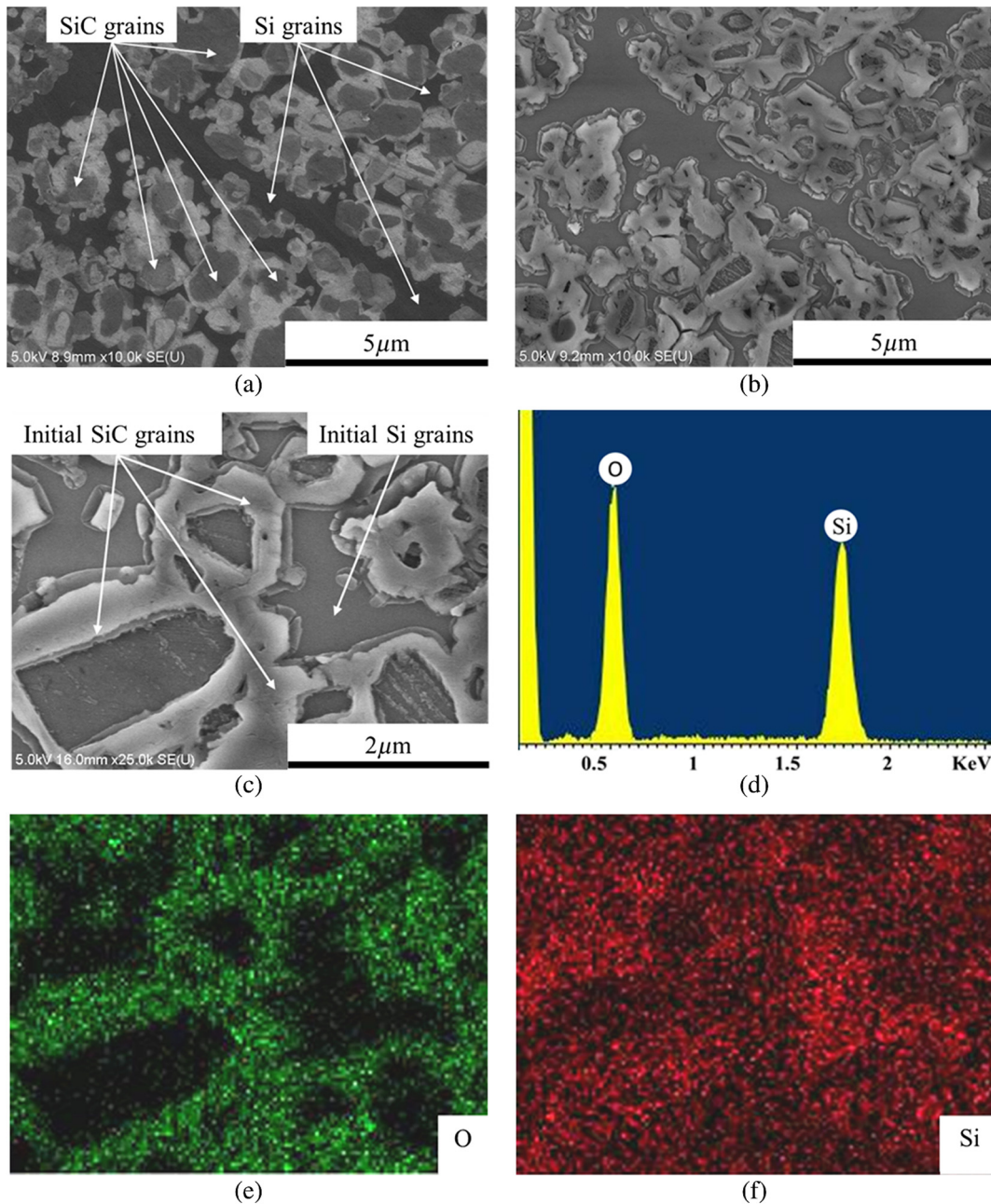


Fig. 2 Morphologies of the oxidized reaction-sintered silicon carbide (RS-SiC) under constant potential mode observed by scanning electron microscope/energy dispersive x-ray spectroscopy (SEM-EDX): (a) original RS-SiC surface; (b) after oxidation at the same position with (a); (c) surface morphology; (d) element analysis; (e) distribution of oxygen; and (f) distribution of silicon.

Fig. 3(e). Therefore, further investigation is needed to verify the detailed differences in the oxide morphologies between the two anodic oxidation modes.

To further investigate the differences of oxide morphologies between the two modes, SEM observation with high magnification has been conducted. The results are shown in Figs. 4 and 5. Under constant potential, there are protuberances and cracks on the oxidized RS-SiC sample, most of which are at the boundaries of the original SiC grains and Si grains, as shown in Fig. 4(b). The protuberances appear at the oxide generated from initial SiC grains, while surfaces of the oxide generated from initial Si grains are relatively

smooth, as shown in Fig. 4(c). The fringe region of a certain SiC grain has a higher oxidation rate relative to the central area, as shown in Fig. 4(d). The reason for this phenomenon could be the asymmetric distribution of the oxidation rate during the oxidation process.³ The oxidation of SiC/Si to SiO₂ is a volume expansion process, which generates the swelling pressure. The distribution of this pressure is determined by the distribution of the oxidation rate. Thus, in the thickness direction, the pressure ejects the oxide, resulting in the formation of protuberances; in the plane direction, the pressure presses the neighboring grains, causing the introduction of cracks in the weak areas. Meanwhile, there are

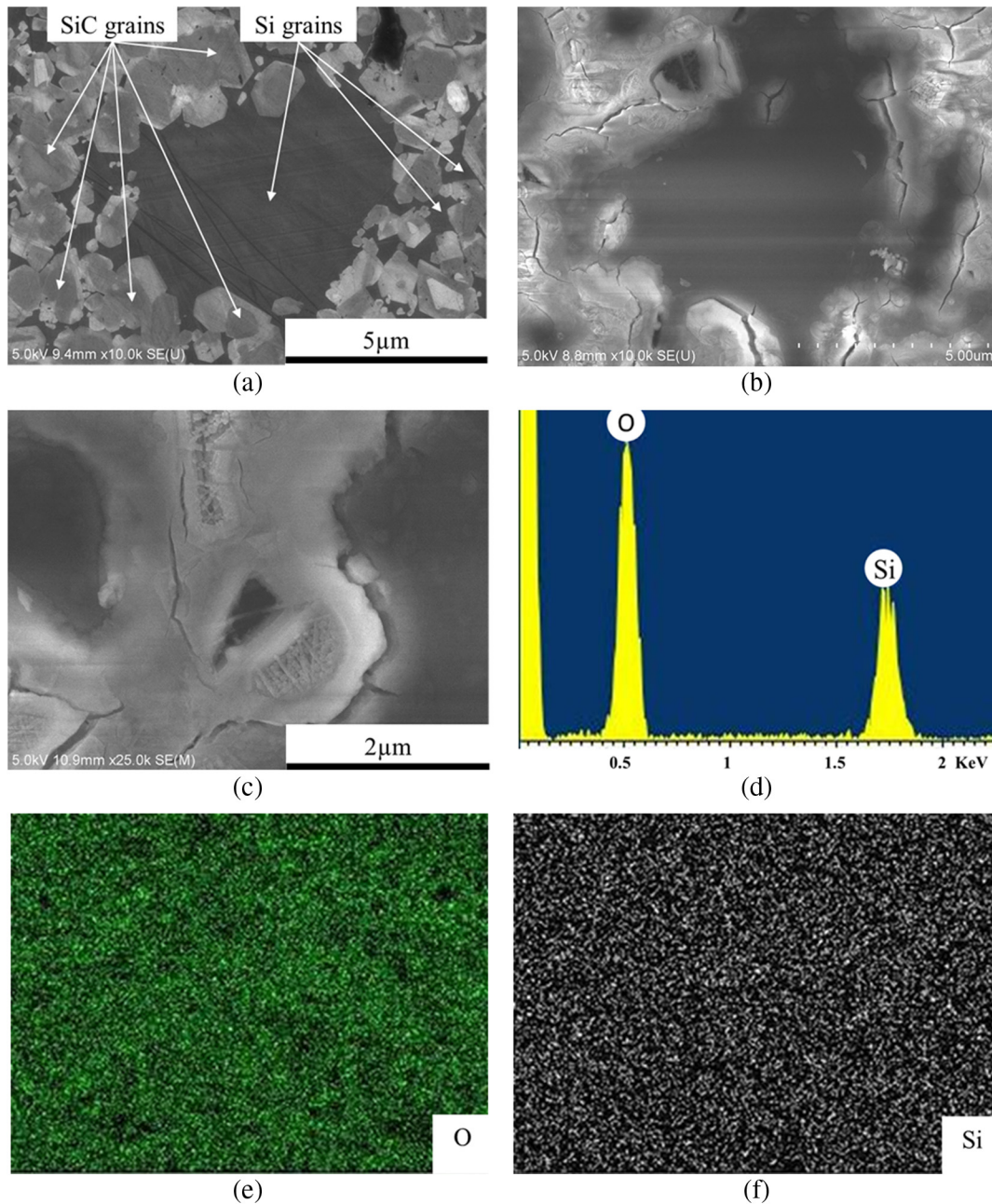


Fig. 3 Morphologies of the oxidized RS-SiC under HFSW potential mode observed by SEM-EDX: (a) original RS-SiC surface; (b) after oxidation at the same position with (a); (c) surface morphology; (d) element analysis; (e) distribution of oxygen; (f) distribution of silicon.

many holes and ditches on the oxidized RS-SiC obtained in the HFSW potential mode, as shown in Fig. 5(a). The width of some ditches reaches 100 nm, as shown in Figs. 5(b) and 5(d), while the radius of some holes reaches 500 nm, as shown in Fig. 5(c). These holes and ditches on the oxidized RS-SiC sample are caused by the unsteady and desultory volume expansion force generated in the HFSW potential mode. Obviously, the ditches and holes on the oxidized RS-SiC obtained in the HFSW potential mode is difficult to remove relative to the protuberances and cracks on that generated in the constant potential mode.

For the purpose of quantificational analysis of the oxidized surface, SWLI measurement is conducted to evaluate

the oxidized samples, as shown in Fig. 6. The surface roughnesses, root mean square (rms), and roughness average (Ra) of the oxidized RS-SiC surface in the constant potential mode are 266.968 and 177.084 nm, while those under HFSW potential are 369.634 and 293.535 nm, respectively. The results indicate that the surface quality of the constant potential case is better than that of the HFSW potential case. Therefore, this study will focus on the anodic oxidation of RS-SiC in the constant potential mode.

4 Calculation of Oxidation Rate

By HF etching of the oxidized RS-SiC samples, the oxide product silica (SiO_2) of RS-SiC can be removed

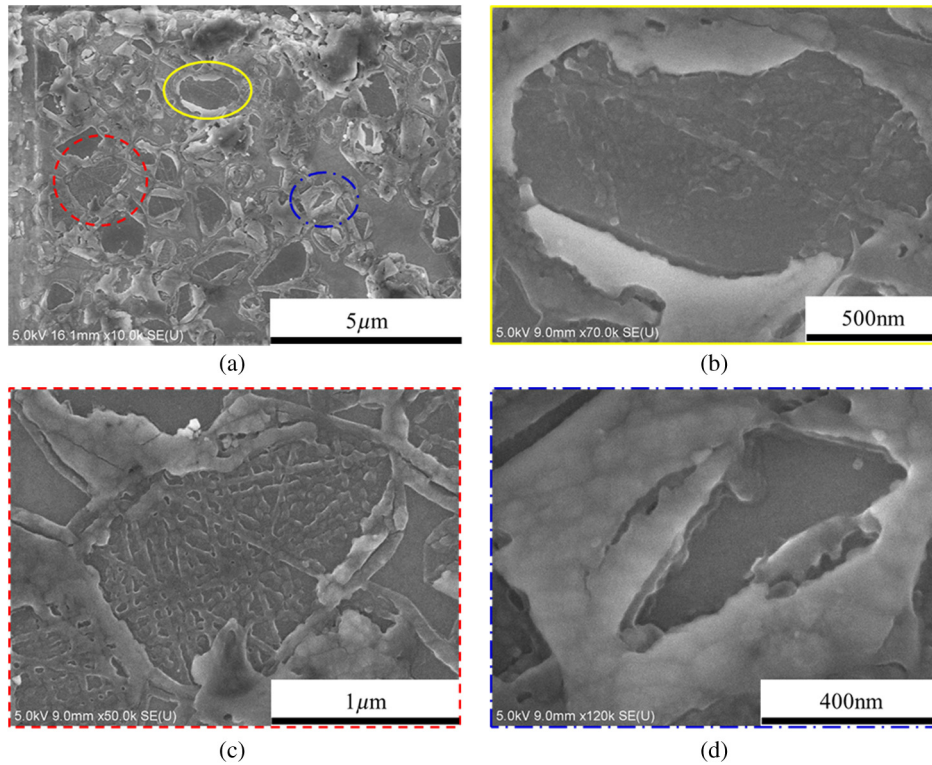


Fig. 4 Oxide morphology under constant potential observed by SEM with high magnification: (a) investigated area; (b) detailed morphologies of region marked by yellow real line in (a); (c) detailed morphologies of region marked by red dashed line in (a); and (d) detailed morphologies of region marked by blue dot-dashed line in (a).

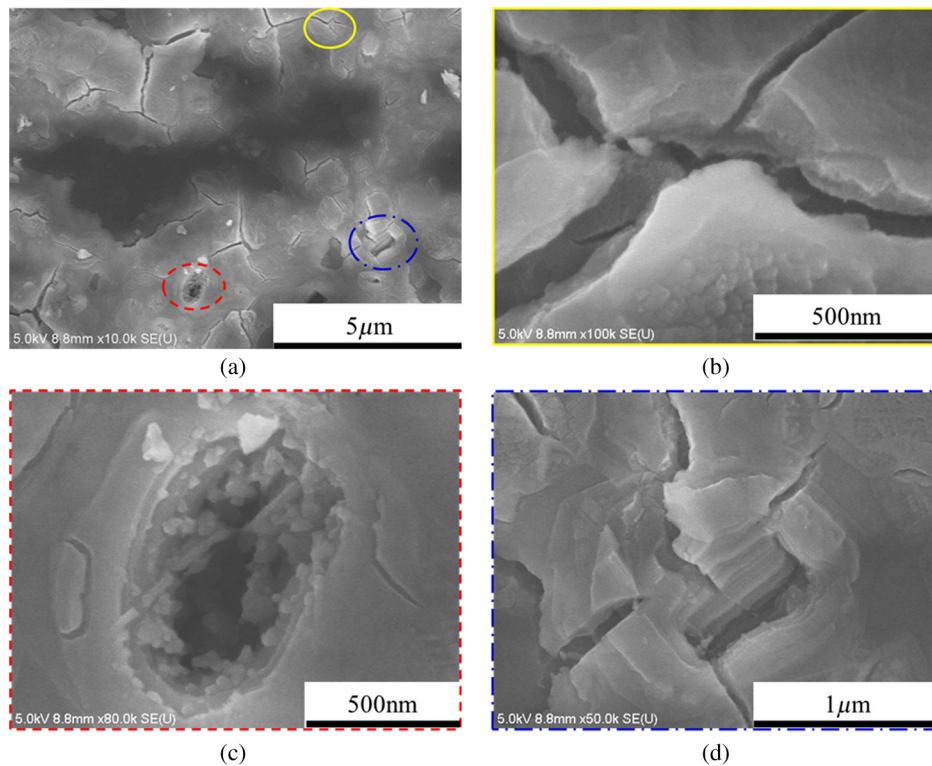


Fig. 5 Oxide morphology under HFSW potential observed by SEM with high magnification: (a) investigated area; (b) detailed morphologies of region marked by yellow real line in (a); (c) detailed morphologies of region marked by red dashed line in (a); and (d) detailed morphologies of region marked by blue dot-dashed line in (a).

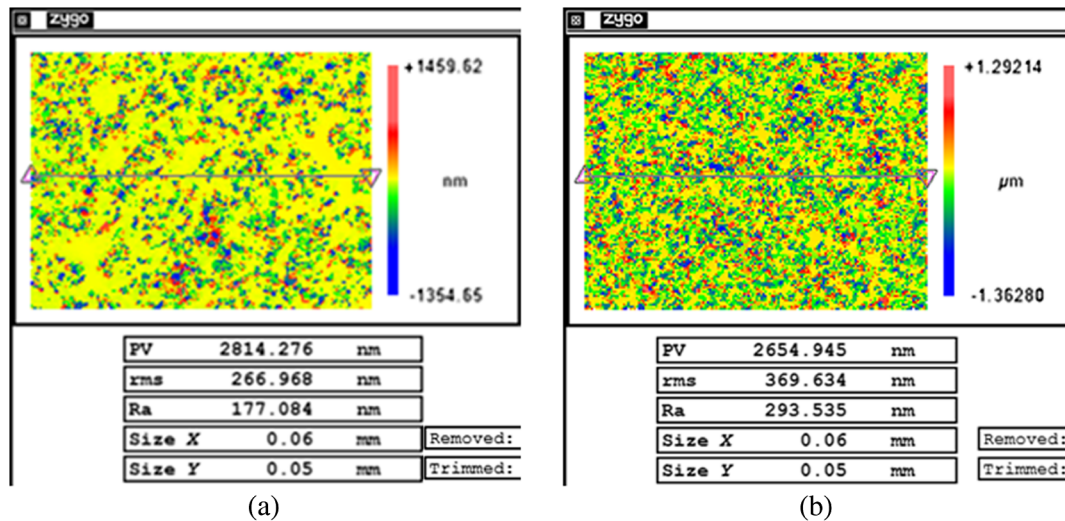
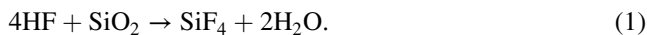


Fig. 6 Quantificational analysis of surface roughness obtained by SWLI measurement: (a) after anodic oxidation under the constant potential and (b) after anodic oxidation under the HFSW potential.

based on the following chemical reaction, as shown in Eq. (1).



Therefore, by comparing surface morphologies of the oxidized RS-SiC samples before and after HF etching, the oxidation depth can be obtained. Experiments were carried out in the constant potential mode with the parameters in Table 1. The measurement results of oxidation depth after a certain oxidation time are shown in Fig. 7. Taking the SWLI measurement result in Fig. 7(a), for example, the oxide SiO_2 in the oxidized area is etched by the HF, which makes a “step” at the boundary region between the oxidized area and the nonoxidized area. By calculating the average height difference of the step, the oxidation depth can be obtained. The calculated anodic oxidation depths are 25, 38, 47, 58, 68, 88, 102, 120, 135, 145, 156, and 163 nm, respectively, and the corresponding oxidation times are 5, 10, 20, 30, 60, 120, 180, 300, 600, 900, 1200, and 1800 s.

For the purpose of calculating the oxidation rate in the constant potential mode according to the classical Deal–Grove model,^{3,15} the relationships between the anodic oxidation depth and the corresponding oxidation time are summarized in Fig. 8. It can be observed that the increasing rate of the oxidation depth reduces when the anodic oxidation time increases. This is because the continuously widened oxide layer counteracts the further occurrence of the oxidation process.

Through data fitting (isolated singularities are filtered) based on the Deal–Grove model,¹⁵ the relationship between the oxidation depth x (nm) and the oxidation time t (s) for anodic oxidation of RS-SiC by H_2O_2 and HCl under the constant potential can be obtained, as shown in Eq. (2).

$$t = 0.01x^2 + 0.19x. \quad (2)$$

If the generated oxide layer by anodic oxidation is removed simultaneously with the abrasive polishing, the oxidation process is kept in the original moment and the quadratic

item in Eq. (2) can be eliminated. Thus, Eq. (2) can be replaced by the linear Deal–Grove model, as shown in Eq. (3).

$$t = 0.19x. \quad (3)$$

Therefore, in the simultaneous anodically oxidation-assisted polishing, in which the anodic oxidation of RS-SiC and the abrasive polishing of oxide layer are carried out at the same time, the theoretical oxidation rate is 5.3 nm/s. In other words, the MRR in this machining process can reach 5.3 nm/s (0.318 $\mu\text{m}/\text{min}$). This MRR is similar to the MRRs obtained from the other rough figuring methods for machining of RS-SiC, and is much larger than those obtained from those fine finishing techniques. Meanwhile, the oxidation depth after oxidation of RS-SiC for 30 min can reach 0.163 μm . Thus, nonsimultaneous anodically oxidation-assisted polishing, in which the abrasive polishing of oxide layer is carried out after the anodic oxidation of RS-SiC, is also a feasible method for machining RS-SiC samples.

5 Investigation of Polishing Property

In order to further investigate the machinability of the oxide layer obtained in anodic oxidation of RS-SiC by the mixture of H_2O_2 and HCl under the constant potential, the oxidized sample is polished with the ceria slurry polishing system, as shown in Fig. 9.³ The reason for applying the ceria slurry polishing method is that it is easier to obtain high MRR and ultrasmooth surface simultaneously in the polishing of silica (SiO_2) by CeO_2 in the chemical mechanical polishing.¹⁶ The oxidized RS-SiC sample is fixed on the stage, while the oxidized surface contacts the ceria slurry. The polishing pad is immersed into the slurry, and the oxidized RS-SiC surface is abraded by the polishing pad. The load is adjusted by changing weights on the load plate. The polishing parameters are summarized in Table 3. The anodic oxidation parameters for the preparation of the oxidized RS-SiC samples are the same as those parameters in Table 1. The anodic oxidation time is 10 min.

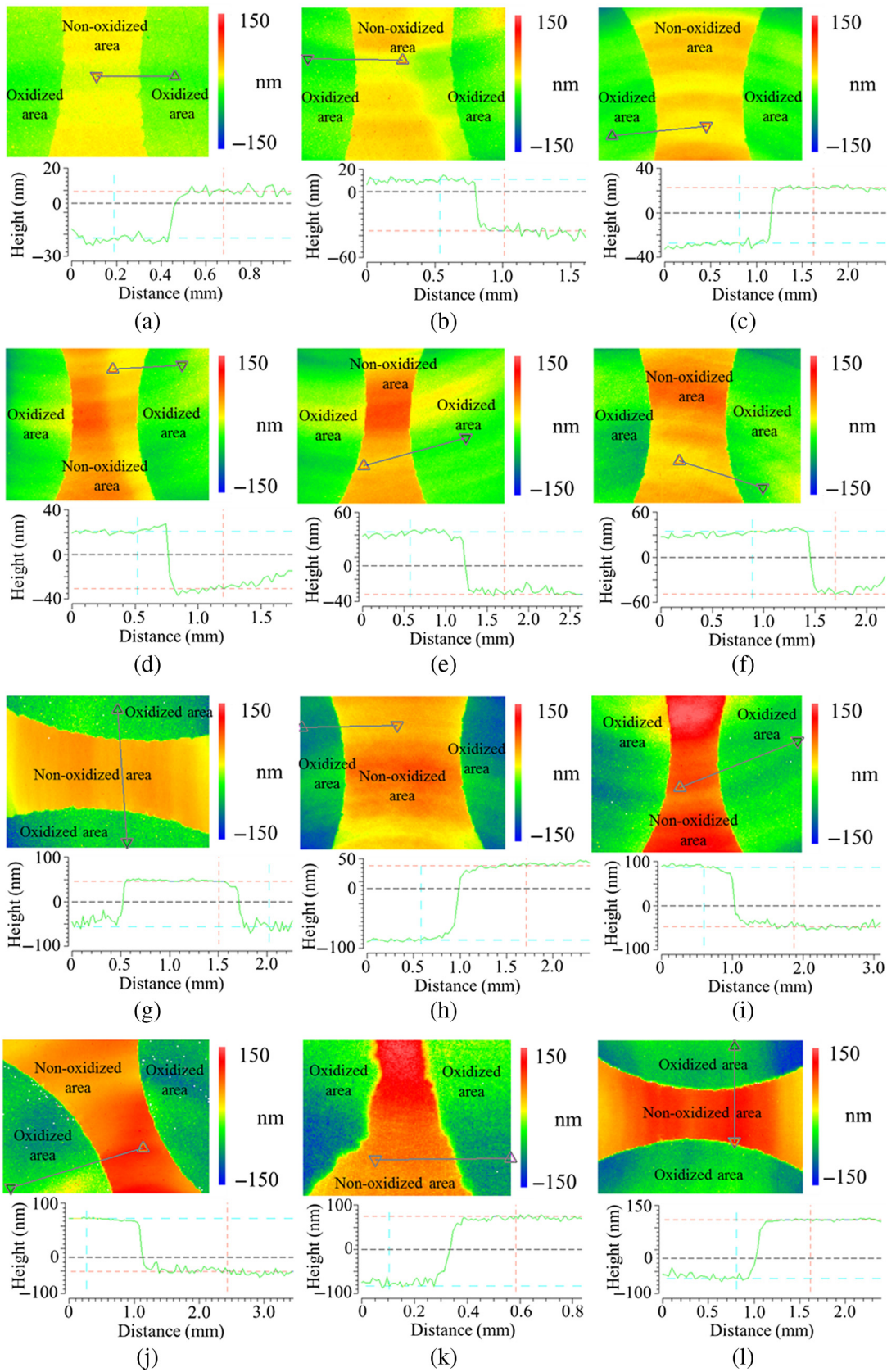


Fig. 7 Calculation of the anodic oxidation depth under the constant potential by SWLI measurement: (a) oxidation for 5 s; (b) oxidation for 10 s; (c) oxidation for 20 s; (d) oxidation for 30 s; (e) oxidation for 60 s; (f) oxidation for 120 s; (g) oxidation for 180 s; (h) oxidation for 300 s; (i) oxidation for 600 s; (j) oxidation for 900 s; (k) oxidation for 1200 s; and (l) oxidation for 1800 s.

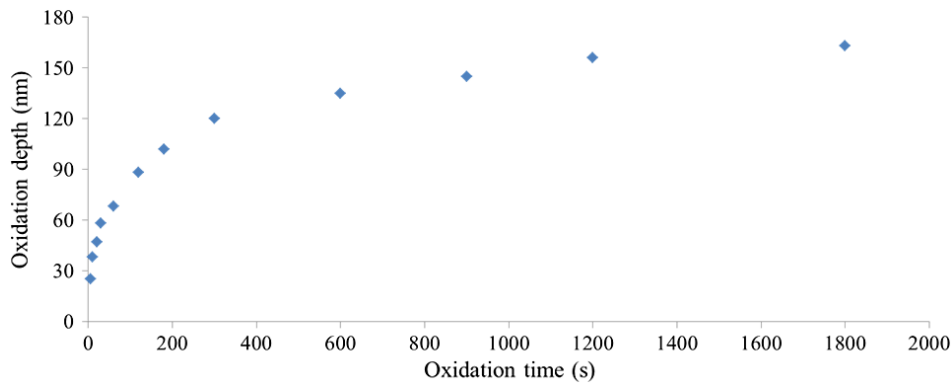


Fig. 8 The relationship between anodic oxidation depth and corresponding oxidation time.

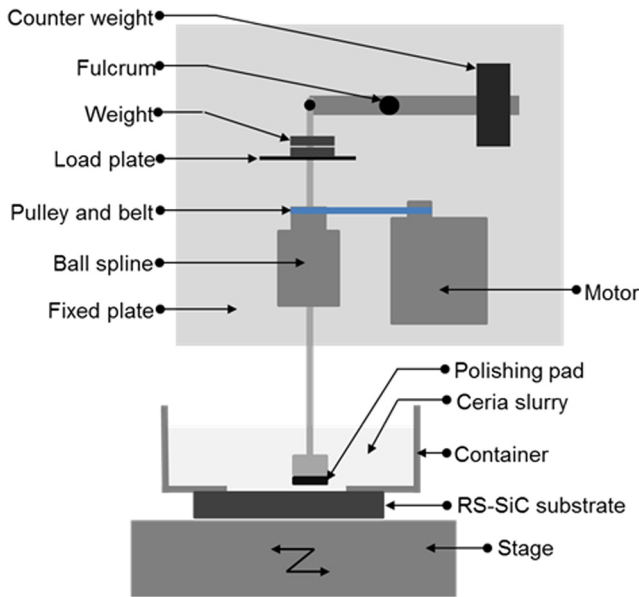


Fig. 9 Schematic diagram of the ceria slurry polishing system.

Table 3 The summarized parameters in ceria slurry polishing of the oxidized RS-SiC sample.

Specimen and its size	Oxidized RS-SiC, 15 mm × 15 mm
Abrasive and its size	Ceria, ϕ 190 nm
Slurry concentration	0.1 wt%
Load and downward pressure	100 g, 12.475 kPa
Rotation speed and scanning speed	300 rpm, 100 mm/ min
Polishing pad and its size	K0017 (FILWEL Co. Ltd.), ϕ 10 mm

During the polishing process, the RS-SiC sample is detected by the SWLI measurement after polishing for a certain time. The obtained data corresponding to an oxidation time from 20 to 240 min at the interval of 20 min is exhibited from Figs. 10(a)–10(l). The relationship between the surface

roughnesses (rms and Ra) and the polishing time is summarized in Fig. 11.

The oxidized RS-SiC surface is very rough, which can be judged from the data in Fig. 6(a). The entire polishing process can be divided into three periods: the removal of protuberances (the first 60 min), the removal of cracks (from 60 to 140 min), and overpolishing (the remaining time). During the period of removing protuberances, the surface roughness rms is rapidly improved to 39.453 nm, because the component of the oxide protuberance is soft SiO₂, which can be easily removed. During the period of removing cracks, the surface roughness rms is improved from 39.453 to 5.002 nm, since most of the cracks penetrate into the inside of the oxide and the MRR in this period is relatively low. During the period of overpolishing, the surface roughness rms stays around 4.5 nm with little undulation, because the oxide has already been removed and the MRR for polishing hard RS-SiC with soft ceria particles is extremely low.

Anodically oxidation-assisted polishing of RS-SiC can obtain a smooth surface with roughness rms around 4.5 nm. Although the surface property is not as good as that obtained with the fine finishing methods, it is obviously better than those obtained with the rough figuring methods, such as PCVM and diamond turning. Moreover, from the calculation of oxidation rate, it can be found that the MRR in simultaneous anodically oxidation-assisted polishing of RS-SiC can reach 0.318 μ m/min, which is close to those in the rough figuring methods and is much larger than those in the fine finishing methods. Therefore, anodically oxidation-assisted polishing can be considered as an efficient processing method, which can fill the performance gap between the rough figuring and fine finishing of RS-SiC.

6 Conclusions

Anodically oxidation-assisted polishing is conducted in this research for efficient machining of RS-SiC. The electrolyte used in anodic oxidation of RS-SiC is a mixture of H₂O₂ and HCl, and the applied potential has two modes: the constant potential and HFSW potential. The oxide morphologies in the two oxidation modes are obtained using SEM-EDX observation and SWLI detection. The comparison results indicate that anodic oxidation under constant potential can not only obtain a smooth surface but also be propitious to achieve high MRR with simultaneous anodically oxidation-assisted polishing. By measuring the anodic oxidation depth with different oxidation times, a theoretical oxidation

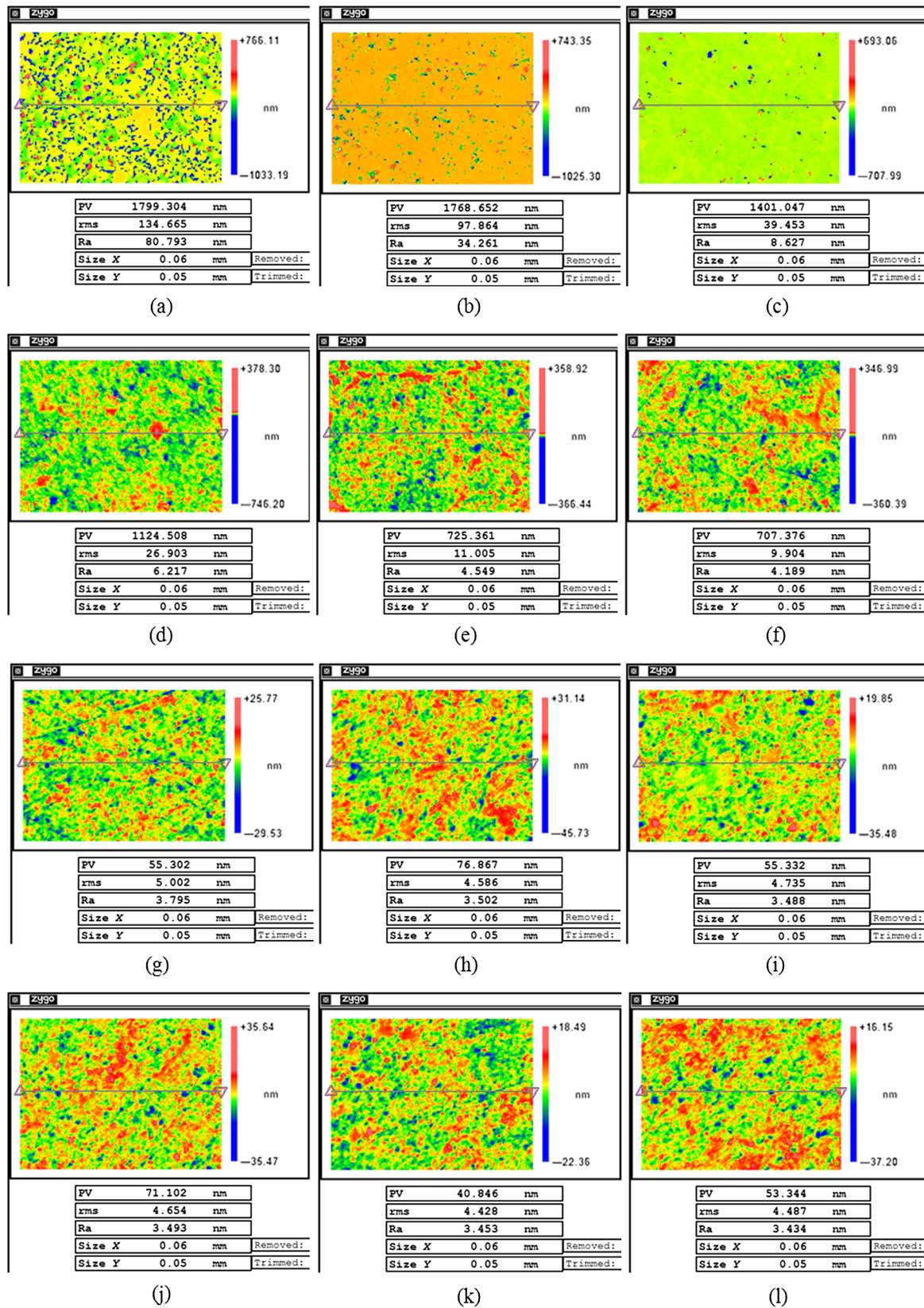


Fig. 10 The summarized surface roughness data obtained by SWLI measurement in the ceria slurry polishing of the oxidized RS-SiC: (a) polishing for 20 min; (b) polishing for 40 min; (c) polishing for 60 min; (d) polishing for 80 min; (e) polishing for 100 min; (f) polishing for 120 min; (g) polishing for 140 min; (h) polishing for 160 min; (i) polishing for 180 min; (j) polishing for 200 min; (k) polishing for 220 min; and (l) polishing for 240 min.

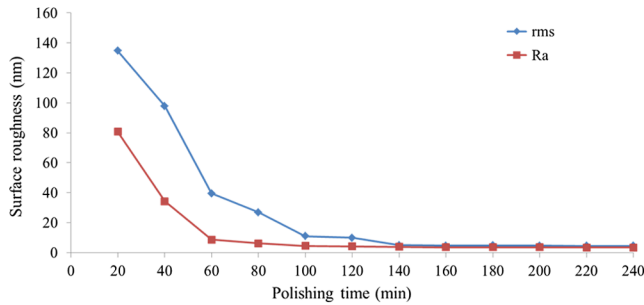


Fig. 11 The relationship between surface roughnesses (rms and Ra) with the corresponding polishing time.

rate based on the linear Deal–Grove model is obtained, which shows that the MRR in simultaneous anodically oxidation-assisted polishing of RS-SiC can reach $0.318 \mu\text{m}/\text{min}$. By ceria slurry polishing of the oxidized RS-SiC, the machinability of the oxide is investigated using the SWLI measurement, and the obtained surface roughness rms is around 4.5 nm . Based on the results in this research, anodically oxidation-assisted polishing can be considered as an efficient processing method, which can fill the performance gap between the rough figuring and fine finishing of RS-SiC. Also, it will improve the processing quality of RS-SiC parts and promote the application of RS-SiC products in the optical and ceramic fields.

Acknowledgments

This work was supported by a grant from the National Natural Science Foundation of China (Grant No. 51505498) and a grant from the Natural Science Foundation of Jiangsu Province (Grant No. BK20150714). The authors also express their gratitude to the staffs and students of the Research Center for Ultra-precision Science and Technology of Osaka University.

References

1. S. Suyama, T. Kameda, and Y. Itoh, "Development of high-strength reaction-sintered silicon carbide," *Diamond Relat. Mater.* **12**(3–7), 1201–1204 (2003).

2. S. Q. Ding et al., "Fabrication of mullite-bonded porous silicon carbide ceramics by in situ reaction bonding," *J. Eur. Ceram. Soc.* **27**(4), 2095–2102 (2007).
3. X. M. Shen et al., "Comparative analysis of oxidation methods of reaction-sintered silicon carbide for optimization of oxidation-assisted polishing," *Opt. Express* **21**(22), 26123–26135 (2013).
4. H. Y. Tam et al., "Removal rate and surface roughness in the lapping and polishing of RB-SiC optical components," *J. Mater. Process. Technol.* **192–193**, 276–280 (2007).
5. H. Zhu et al., "Rapid fabrication of lightweight SiC mirror using CCOS," *Proc. of SPIE* **8194**, 81942A (2011).
6. Z. Y. Zhang, J. W. Yan, and T. Kuriyagawa, "Study on tool wear characteristics in diamond turning of reaction bonded silicon carbide," *Int. J. Adv. Manuf. Technol.* **57**(1–4), 117–125 (2011).
7. J. Yan, Z. Zhang, and T. Kuriyagawa, "Mechanism for material removal in diamond turning of reaction-bonded silicon carbide," *Int. J. Mach. Tools Manuf.* **49**(5), 366–374 (2009).
8. K. Yamamura, Y. Yamamoto, and H. Deng, "Preliminary study on chemical figuring and finishing of sintered sic substrate using atmospheric pressure plasma," *Procedia CIRP* **3**, 335–339 (2012).
9. X. M. Shen et al., "Mechanism analysis on finishing of reaction-sintered silicon carbide by combination of water vapor plasma oxidation and ceria slurry polishing," *Opt. Eng.* **54**(5), 055106 (2015).
10. O. P. Chakrabarti, P. K. Das, and J. Mukerji, "Growth of SiC particles in reaction sintered SiC," *Mater. Chem. Phys.* **67**(1–3), 199–202 (2001).
11. X. M. Shen et al., "Ultrasmooth reaction-sintered silicon carbide surface resulting from combination of thermal oxidation and ceria slurry polishing," *Opt. Express* **21**(12), 14780–14788 (2013).
12. C. H. Li et al., "Electro-chemical mechanical polishing of silicon carbide," *J. Electron. Mater.* **5**(33), 481–486 (2007).
13. W.S. Woon et al., "Characterization of anodic SiO_2 films on P-type 4H-SiC," *Thin Solid Films* **517**(8), 2808–2812 (2009).
14. Y. Ke et al., "Surface polishing by electrochemical etching of p-type 4H SiC," *J. Appl. Phys.* **106**, 064901 (2009).
15. B. E. Deal and A. S. Grove, "General relationship for the thermal oxidation of silicon," *J. Appl. Phys.* **36**, 3770–3778 (1965).
16. W. Q. Peng, C. L. Guan, and S. Y. Li, "Material removal mechanism of ceria particles with different sizes in glass polishing," *Opt. Eng.* **53**(3), 035104 (2014).

Xinmin Shen is a lecturer at PLA University of Science and Technology. He received his BS, MS, and PhD degrees in Mechanical Engineering from National University of Defense Technology (NUDT) in 2008, 2010, and 2014, respectively. He had studied in Osaka University from 2011 to 2013 as a special research student. He is the author of more than 20 papers. His current research focuses on the ultraprecision machining of optical components.

Biographies for the other authors are not available.